Transplantation of Glial Progenitors That Overexpress Glutamate Transporter GLT1 Preserves Diaphragm Function Following Cervical SCI

Ke Li[1], Elham Javed[1], Tamara J Hala[1], Daniel Sannie[1], Kathleen A Regan[1], Nicholas J Maragakis[2], Megan C Wright[3], David J Poulsen[4] and Angelo C Lepore[1]

[1]Department of Neuroscience, Farber Institute for Neurosciences, Sidney Kimmel Medical College at Thomas Jefferson University, Philadelphia, Pennsylvania, USA; [2]Department of Neurology, Johns Hopkins University School of Medicine, Baltimore, Maryland, USA; [3]Department of Biology, Arcadia University, Glenside, Pennsylvania, USA; [4]Department of Biomedical and Pharmaceutical Sciences, University of Montana, Missoula, Montana, USA

Approximately half of traumatic spinal cord injury (SCI) cases affect cervical regions, resulting in chronic respiratory compromise. The majority of these injuries affect midcervical levels, the location of phrenic motor neurons (PMNs) that innervate the diaphragm. A valuable opportunity exists following SCI for preventing PMN loss that occurs during secondary degeneration. One of the primary causes of secondary injury is excitotoxicity due to dysregulation of extracellular glutamate homeostasis. Astrocytes express glutamate transporter 1 (GLT1), which is responsible for the majority of CNS glutamate clearance. Given our observations of GLT1 dysfunction post-SCI, we evaluated intraspinal transplantation of Glial-Restricted Precursors (GRPs)—a class of lineage-restricted astrocyte progenitors—into ventral horn following cervical hemicontusion as a novel strategy for reconstituting GLT1 function, preventing excitotoxicity and protecting PMNs in the acutely injured spinal cord. We find that unmodified transplants express low levels of GLT1 in the injured spinal cord. To enhance their therapeutic properties, we engineered GRPs with AAV8 to overexpress GLT1 only in astrocytes using the GFA2 promoter, resulting in significantly increased GLT1 protein expression and functional glutamate uptake following astrocyte differentiation *in vitro* and after transplantation into C4 hemicontusion. Compared to medium-only control and unmodified GRPs, GLT1-overexpressing transplants reduced lesion size, diaphragm denervation and diaphragm dysfunction. Our findings demonstrate transplantation-based replacement of astrocyte GLT1 is a promising approach for SCI.

Received 27 August 2014; accepted 2 December 2014; advance online publication 6 January 2015. doi:10.1038/mt.2014.236

INTRODUCTION

Significant and often chronic respiratory compromise is a major cause of morbidity and mortality following traumatic cervical spinal cord injury (SCI). Cervical SCI represents greater than half of all human cases, in addition to often resulting in the most severe physical and psychological debilitation.[1] Phrenic motor neuron (PMN) loss plays a central role in this respiratory compromise. The diaphragm, a major inspiratory muscle, is innervated by PMNs located at cervical levels 3–5,[2] and PMN output is driven by descending premotor bulbospinal neurons in the medullary ventral respiratory group (VRG).[3] Cervical SCI results in respiratory compromise due to PMN loss and/or injury to descending bulbospinal respiratory axons. The majority of these injuries affect midcervical levels[4] (the location of the PMN pool), and respiratory function following midcervical SCI is significantly determined by PMN loss/sparing.[5]

Initial spinal cord trauma results in immediate cell death and axotomy of passing fibers. Contusion-type injury, the predominant form of traumatic SCI observed in the clinical population, is followed by an extended period of secondary cell death and consequent exacerbation of functional deficits.[6] One of the major causes of secondary degeneration is excitotoxicity due to dysregulation of extracellular glutamate homeostasis.[7] A valuable opportunity therefore exists following cervical SCI for preventing PMN loss that occurs during secondary degeneration, as well as consequently preserving respiratory function.

Glutamate is efficiently cleared from the synapse and other sites by transporters located on the plasma membrane.[8] Astrocytes express glutamate transporter 1 (GLT1), which is responsible for the vast majority of functional glutamate uptake and plays a central role in regulation of extracellular glutamate homeostasis in spinal cord.[9] We previously found that in rodent models of unilateral midcervical (C4) hemicontusion, numbers of GLT1-expressing astrocytes and total intraspinal GLT1 protein expression in ventral horn are reduced soon after injury and persist chronically, resulting in further susceptibility to excitotoxicity.[10]

Transplantation-based replacement of lost and/or dysfunctional astrocytes is a promising approach for SCI. However, neural stem/progenitor cell transplantation strategies have not been extensively explored in SCI models for targeting neuroprotective astrocyte functions (such as GLT1-mediated glutamate uptake),[11] despite the fact that astrocytes play a host of integral homeostatic roles in the adult CNS.[12]

Correspondence: *Angelo C Lepore, Department of Neuroscience, Farber Institute for Neurosciences, Sidney Kimmel Medical College at Thomas Jefferson University, 900 Walnut Street, JHN 469, Philadelphia, Pennsylvania, USA. E-mail: angelo.lepore@jefferson.edu*

We previously showed that GRP transplant-derived astrocytes express GLT1 and attenuate intraparenchymal loss of GLT1 protein expression in cervical spinal cord of the transgenic SOD1^{G93A} model of ALS, resulting in therapeutic protection of PMNs, preservation of diaphragm function and extension in overall disease.[13] These previous findings suggest the feasibility of transplantation-based astrocyte replacement as a therapeutic strategy for restoring intraparenchymal GLT1 function and consequently preventing focal PMN loss in the diseased spinal cord.

In this study, we tested intraspinal transplantation of Glial-Restricted Precursors (GRPs)—a class of lineage-restricted astrocyte progenitors[14]—into ventral horn following C4 hemicontusion SCI as a novel therapeutic strategy for transplantation-based delivery of astrocytes to the acutely injured spinal cord, reconstituting GLT1 function, preventing excitotoxicity, and consequently protecting PMNs and preserving diaphragmatic respiratory function.

RESULTS

Transplanted glial progenitor-derived astrocytes do not express GLT1 in the injured cervical spinal cord

Using BAC-GLT1-eGFP transgenic mouse, we previously showed that intraspinal GLT1 expression and GLT1-mediated glutamate uptake by endogenous astrocytes are significantly reduced in SCI,[15] including in the ventral horn following cervical hemicontusion.[10] To efficiently track the *in vivo* spatiotemporal expression of GLT1 by transplanted cells, we derived $A_2B_5^+$ GRP cultures from the same transgenic mouse.[16] The use of the BAC-GLT1 reporter allows for cell-specific quantification of GLT1 expression *in vivo*, which is technically challenging to do with GLT1 immunohistochemistry given the diffuse distribution of GLT1 protein through the CNS, particularly in grey matter. Following *in vitro* differentiation and culturing with neuronal-conditioned medium to stimulate GLT1 expression,[17] GRP-derived astrocytes expressed both GLT1 protein and the BAC-GLT1-eGFP reporter (**Figure 1a**), whereas GLT1 protein and BAC-GLT1-eGFP reporter expression were not observed in undifferentiated GRPs or in GRP-derived astrocytes without the addition of neuronal-conditioned medium (data not shown).

Following transplantation of undifferentiated GRPs into the uninjured cervical spinal cord, graft differentiation and GLT1 expression were examined at week 5 after injection. The mouse-specific marker, M2, was used to identify transplant-derived cells of mouse origin in the host rat spinal cord. M2$^+$ cells survived robustly in both ventral horn gray matter (**Figure 1b**) and surrounding white matter (**Figure 1e**). In addition, a significant percentage of transplant-derived cells expressed GLT1 in both gray (**Figure 1c,d**) and white matter (**Figure 1f,g**) areas. Transplant-derived cells elaborated mature astrocyte-like morphology (**Figure 1h**) and expressed the astrocyte-specific marker, GFAP (**Figure 1i,j**).

In previous studies, we have shown that PMN loss occurs mostly within the first 48 hours after injury.[18] To deliver cells within this therapeutic window, as well as to target secondary degenerative events as early as possible to maximize potential efficacy, we transplanted cells immediately postcontusion in all experiments in this study. To examine the expression of GLT1 at both the injury site and in surrounding locations where overt tissue damage is not observed, cells were transplanted into the same animals at two locations (**Figure 2a**): (i) into the hemicontusion site and (ii) into an adjacent site at level C5 (one spinal segment below and contralateral to the injury site). In order to study the temporal progression of GLT1 expression in the context of SCI, we assessed fate of both transplanted undifferentiated GRPs and GRP-derived astrocytes at multiple time points after injury. Before transplantation, BAC-GLT1-eGFP cells were labeled for tracking and quantification with the retrovirus pMXs-mRFP1 reporter (which was expressed by all cells regardless of lineage) as RFP allows for easier quantification of double-labeling than M2. RFP labeling allowed us to track the expression of GLT1 in transplant-derived GFAP+ astrocytes (**Figure 2b**). Both GRP and GRP-derived astrocyte transplants survived robustly at both the injury site and caudal C5 location in all animals at 2 days, 2 weeks, and 5 weeks after injury (**Figure 2c,d**). In the caudal C5 spinal cord, the majority of transplant-derived cells in both groups expressed GLT1 (detected by the BAC-GLT1-eGFP reporter) at 5 weeks after injection (**Figure 2e**). However, the percentage of cells expressing GLT1 was significantly lower at early time points. Following transplantation of undifferentiated GRPs, only 10% of cells expressed GLT1 at 2 days, and still only 30% of cells expressed GLT1 by 2 weeks. Predifferentiation of GRPs into astrocytes prior to transplantation increased these percentages at both 2 days and 2 weeks; nevertheless, only 30% of cells expressed GLT1 at 2 days (**Figure 2e**). The expression of GLT1 was even lower in transplant-derived cells at the injury site (**Figure 2f**). Approximately, only 10% of cells expressed GLT1 at all three times points, and predifferentiation into astrocytes prior to injection did not increase this percentage.

AAV8-GLT1 transduction *in vitro* increases GLT1 protein expression and GLT1-mediated functional glutamate uptake without compromising normal astrocyte differentiation

To enhance the ability of GRP transplants to modulate extracellular glutamate levels and enhance their *in vivo* therapeutic potential,[19] we engineered GRPs *in vitro* with an AAV8-GFA2-GLT1 vector to overexpress GLT1 only in astrocytes using the astrocyte-specific GFA2 promoter. Following transduction with AAV8-GFA2 control vector, little-to-no expression of GLT1 was noted *in vitro* with either undifferentiated GRPs (**Figure 3a**) or following differentiation into GFAP$^+$ astrocytes using BMP-4 (**Figure 3b**). In addition, GLT1 expression was not observed in undifferentiated GRPs following transduction with AAV8-GFA2-GLT1 vector (data not shown), demonstrating that GLT1 overexpression was not being driven in nonastrocyte cells because of the astrocyte lineage specificity of the GFA2 promoter. On the contrary, a significant increase in the percentage of cells expressing GLT1 protein (**Figure 3c**), overall GLT1 protein expression (**Figure 3d**) and functional GLT1-mediated glutamate uptake (**Figure 3e**) was observed in GRP-derived astrocytes *in vitro* with AAV8-GFA2-GLT1 transduction. Importantly, viral-based GLT1 overexpression did not affect normal astrocyte differentiation (**Figure 3c**) or morphology (**Figure 3b**) *in vitro*.

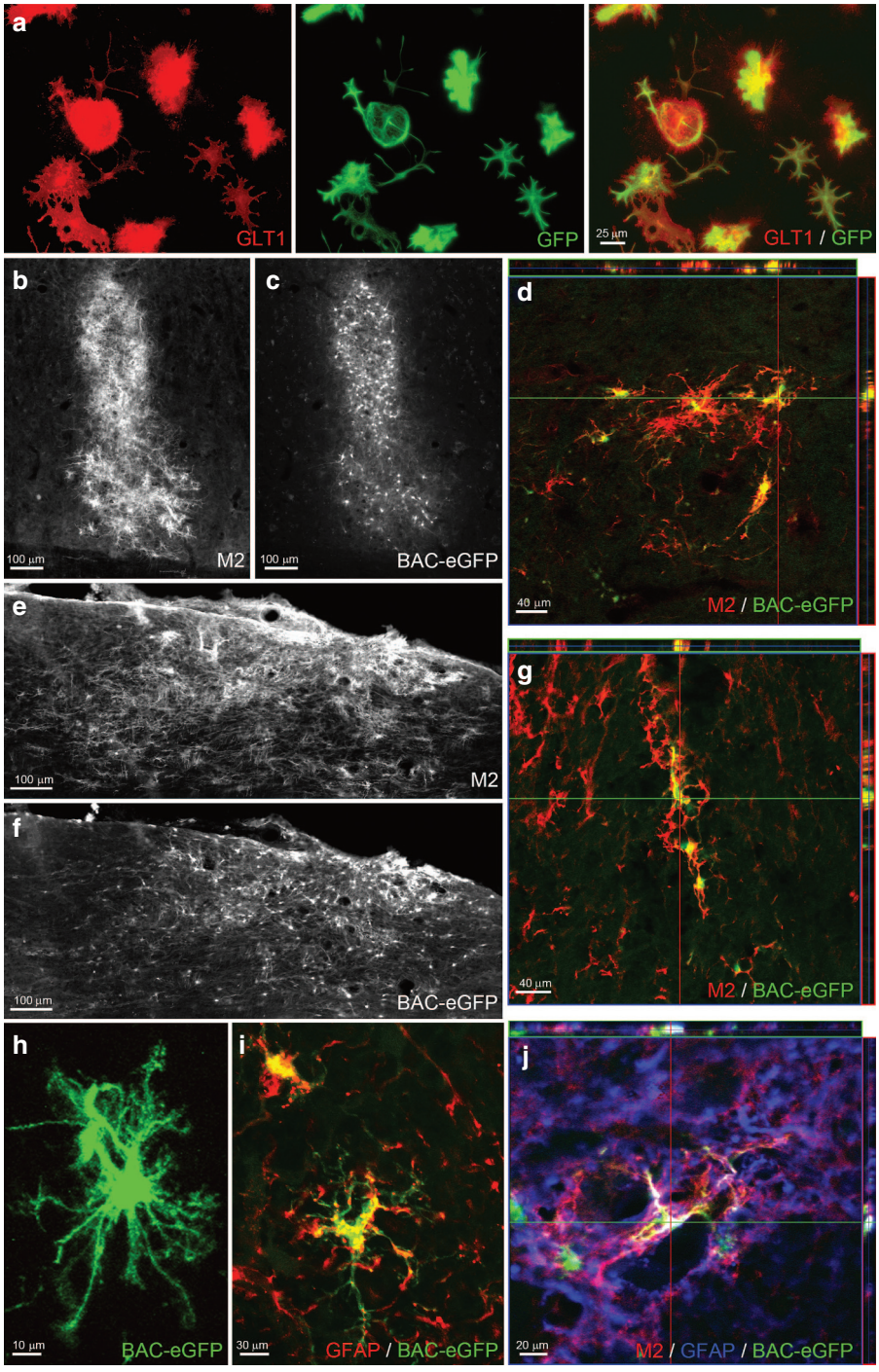

Figure 1 BAC-GLT1-eGFP reporter cells can be used to spatiotemporally track GLT1 expression by transplants in the spinal cord. (**a**) BAC-GLT1-eGFP GRP-derived astrocytes expressed both GLT1 protein and BAC-GLT1-eGFP reporter when cultured with neuronal-conditioned medium. At 5 weeks after transplantation of undifferentiated BAC-GLT1-eGFP GRPs into the uninjured spinal cord, we detected surviving cells in host rat spinal cord with the mouse-specific marker, M2 (**b**: ventral horn gray matter; **e**: surrounding white matter). $M2^+$ transplant-derived cells expressed BAC-GLT1-eGFP reporter in (**c**) gray matter ((**d**) confocal image) and (**f**) white matter ((**g**) confocal image). BAC-GLT1-$eGFP^+$ cells (**h**) elaborated astrocyte-like morphology and (**i**,**j**) expressed GFAP.

GLT1 overexpression significantly enhances GLT1 protein expression by transplanted astrocytes in the injured cervical spinal cord

To test whether AAV8-based overexpression results in increased levels of GLT1 expression, as well as expression at early time points after injection, we transplanted GRP-derived astrocytes immediately post-C4 hemicontusion SCI. Given our observation of accelerated GLT1 expression *in vivo* with the BAC-GLT1-eGFP GRP transplants, we only tested predifferentiated GRP-derived astrocyte transplants in all subsequent experiments. Furthermore, we did not employ cells derived from the BAC-GLT1-eGFP mouse for these transplants. Instead, GRPs

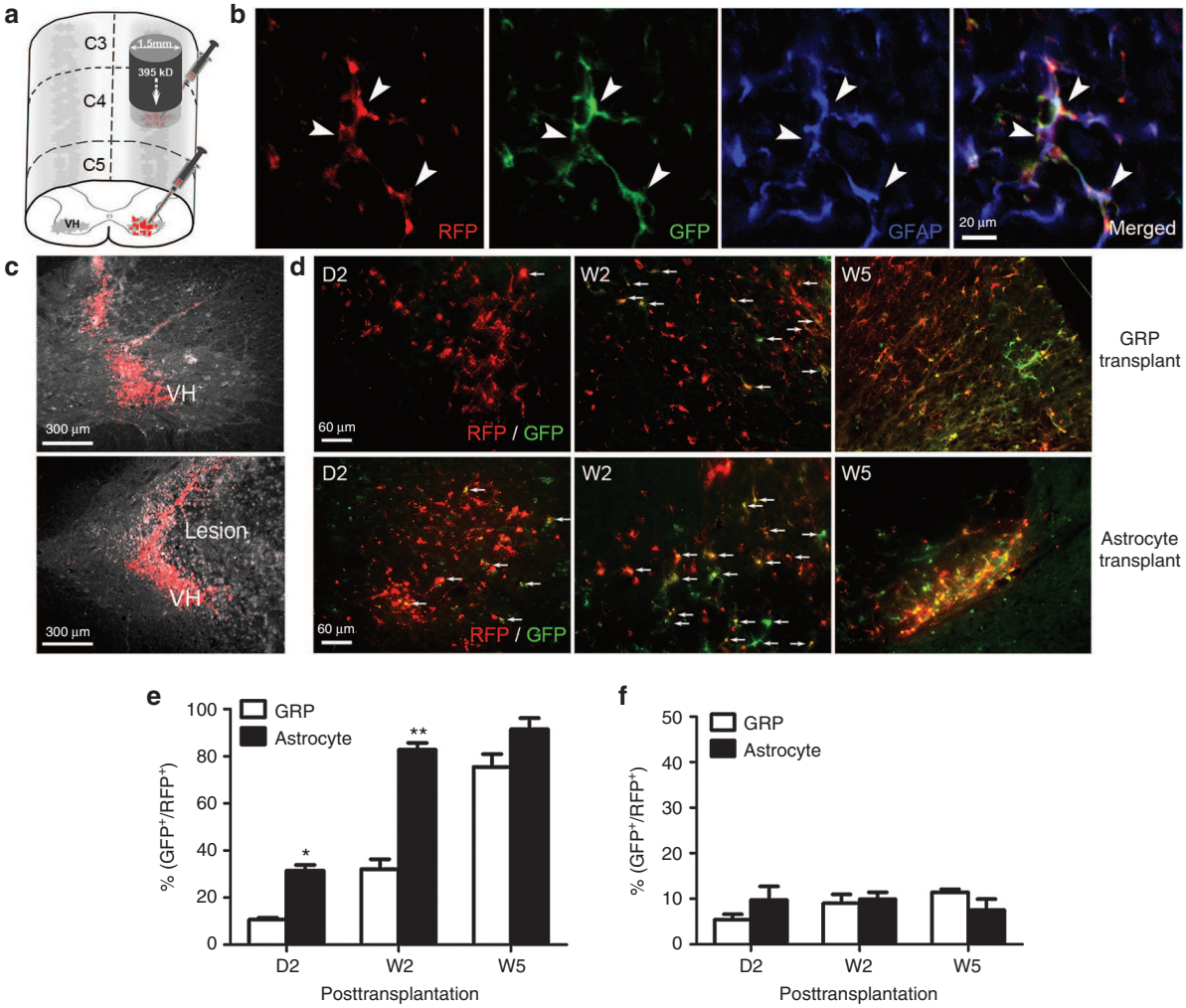

Figure 2 Transplanted glial progenitor-derived astrocytes do not express GLT1 in the injured cervical spinal cord. (**a**) Undifferentiated BAC-GLT1-eGFP GRPs and GRP-derived astrocytes were transplanted into the injured spinal cord, (**c**) where they survived in both the C4 lesion site (lower panel) and surrounding C5 tissue where tissue damage was not observed (upper panel). (**b**) RFP reporter labeling allowed us to track the expression of the BAC-GLT1-eGFP reporter in transplant-derived GFAP$^+$ astrocytes. (**d**) At day 2 (D2), week 2 (W2), and W5 after transplantation, transplant survival (RFP$^+$) and GLT1 expression (BAC-GLT1-eGFP$^+$) were detected in both caudal C5 and intralesion (data not shown) locations. Percentage of GLT1 expressing transplant-derived cells (% of RFP$^+$ cells that are BAC-GLT1-eGFP$^+$) was quantified for transplants of both BAC-GLT1-eGFP undifferentiated GRPs and GRP-derived astrocytes ((**e**) surrounding intact tissue; (**f**) lesion site). Results were expressed as means ± SEM. *$P < 0.05$, **$P < 0.01$, $n = 6$ per group.

were derived from wild-type Sprague-Dawley rats to avoid xenograft issues.

In addition, for all subsequent experiments, we employed a transplantation paradigm that differs from that used in the BAC-GLT1-eGFP GRP studies in an attempt to achieve maximal therapeutic benefit in the unilateral C4 hemicontusion model with respect to obtaining PMN protection and preservation of diaphragm function. Based on the distribution of GRP transplant-derived cells from a single injection site in preliminary studies, the rostral-caudal extent of the lesion with our C4 hemicontusion model, and the rostral-caudal extent of the PMN pool,[13] we transplanted cells into the ventral horn at three total injection locations ipsilateral to the contusion site: directly into the lesion epicenter (one injection of 1.0×10^6 cells), as well as one-half segment rostral and caudal to the epicenter (two injections of 0.5×10^6 cells/each). In this way, we aimed to achieve efficient spatial distribution of cells throughout the area of PMN degeneration.

We compared three injection groups: (i) GRP basal medium-only control; (ii) GRP-derived astrocytes transduced prior to transplantation with AAV8-GFA2 control vector; (iii) GRP-derived astrocytes transduced prior to transplantation with AAV8-GFA2-GLT1 vector. Both cell groups were also transduced with lentiviral vector for labeling of all cells (regardless of their phenotype) with a GFP reporter.

Similar to our results with BAC-GLT1-eGFP GRP transplants, we observed robust survival in the injured spinal cord with both transplant groups out until at least 5 weeks after injury (*i.e.*, the latest time point examined) (**Figure 4**). In addition, 80–90% of transplant-derived cells expressed the astrocyte-specific marker, GFAP (**Figure 4a**,**d**). However, the control transplants expressed very low levels of GLT1 protein both at 10 days (**Figure 4b**) and 5 weeks (**Figure 4c**), while the overexpressing transplants expressed greatly increased levels of GLT1 protein in the injured spinal cord (**Figure 4b**,**c**). Importantly, this high level of GLT1 expression was

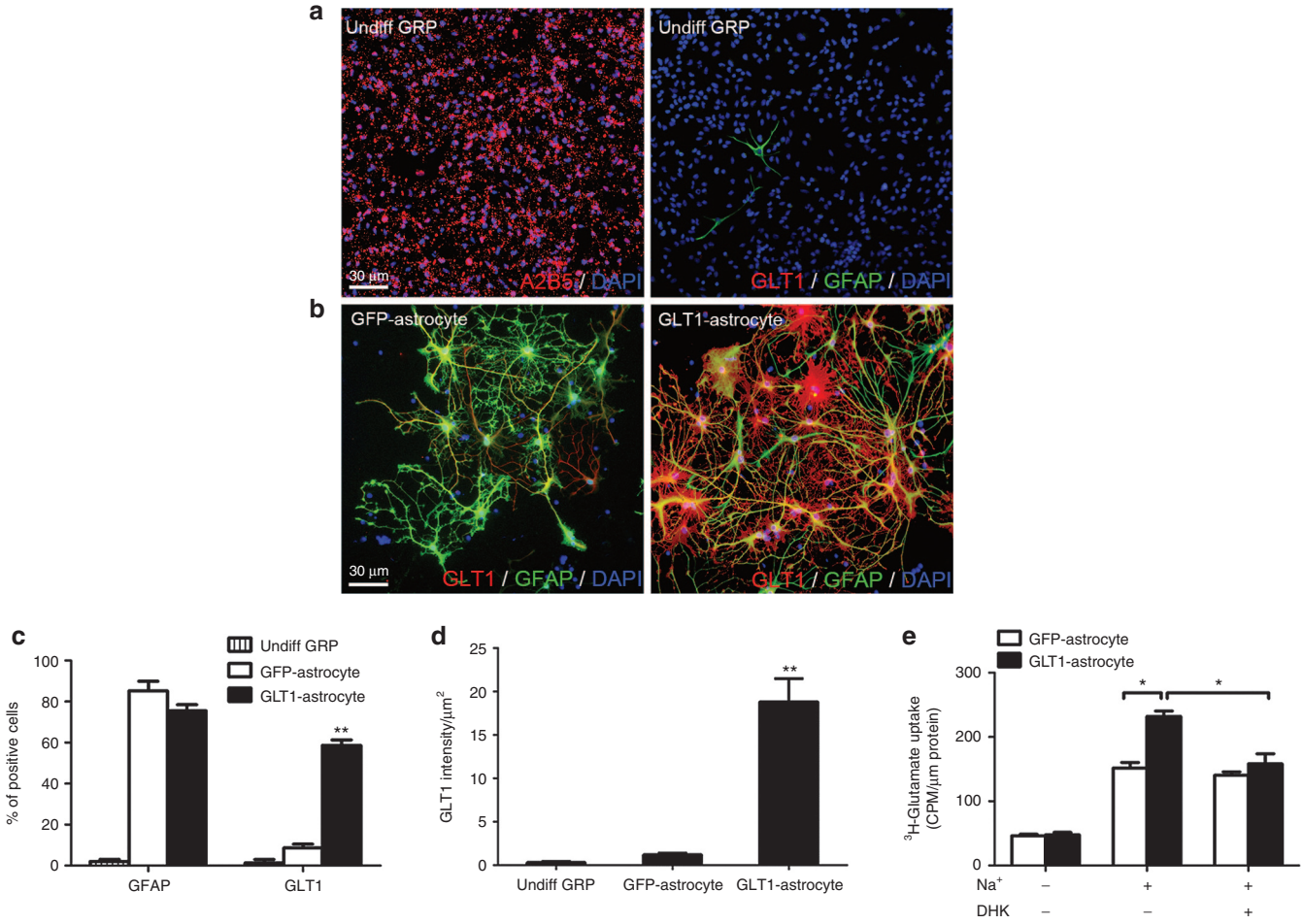

Figure 3 AAV8-GLT1 transduction *in vitro* increases GLT1 protein expression and GLT1-mediated functional glutamate uptake. (**a**) Undifferentiated rat GRPs expressed the glial progenitor marker A_2B_5 (left panel), but not the astrocyte marker GFAP (right panel) *in vitro*. Cultured undifferentiated rat GRPs (right panel) expressed little-to-no GLT1 protein. (**b**) During GRP differentiation into GFAP$^+$ astrocytes, cells transduced with AAV8-Gfa2-GLT1 significantly increased GLT1 protein overexpression (right panel), while cells transduced with AAV8-Gfa2 control vector did not express GLT1 (left panel). (**c**) Percentage of DAPI$^+$ cells *in vitro* expressing GFAP and GLT1 protein. (**d**) Quantification of GLT1 protein expression level *in vitro*. (**e**) *In vitro* ^{3}H-glutamate uptake assay was performed to detect functional Na^+-dependent GLT1-mediated glutamate uptake in GRP-derived astrocytes using the GLT1 inhibitor DHK. Results were expressed as means ± SEM. $^*P < 0.05$, $^{**}P < 0.01$, $n = 6$ per group for GLT1 and GFAP expression analyses, $n = 3$ per group for ^{3}H-glutamate uptake assay.

also observed at the early time point of 10 days after injury/injection (**Figure 4b**). These results were quantified for both transplant groups at both time points (**Figure 4e**). In addition, these GLT1 overexpressing GRP-derived astrocytes were spatially localized around PMNs that were selectively identified via retrograde labeling from the ipsilateral hemidiaphragm with the tracer cholera toxin B (**Figure 4f**), placing the cells in the appropriate location for protecting PMNs.

GLT1 overexpressing astrocyte transplants reduce lesion size following cervical contusion SCI

To test the therapeutic efficacy of GLT1 overexpressing transplants in the unilateral cervical hemicontusion model, we quantified lesion size and total motor neuron sparing. At 10 days after injury, Cresyl-violet stained transverse sections of the cervical spinal cord surrounding the injury site were quantified for the degree of ipsilesional tissue sparing by calculating the percentage of total ipsilateral hemicord area comprised of damaged tissue (**Figure 5a**). Lesion area (**Figure 5b**) and total lesion volume (**Figure 5c**) analysis (combined for both white and gray matter) revealed that GLT1 overexpressing transplants significantly reduced lesion area at multiple locations surrounding the epicenter compared to both medium-only and control transplant groups. This protective effect was observed specifically at points within 1 mm rostral and caudal of the epicenter where the greatest tissue damage occurred. In addition, total α motor neuron loss in the ipsilateral ventral horn was significantly reduced in the GLT1 overexpressing group compared to the two control groups at a number of locations surrounding the lesion epicenter (**Figure 5d**). We did not quantify the preservation of other important neuronal populations of the cervical spinal relevant to diaphragm function such as respiratory interneurons.

GLT1 overexpressing astrocyte transplants preserve diaphragm innervation by phrenic motor neurons following cervical contusion SCI

We found that GLT1 overexpressing transplants significantly preserved morphological innervation at the diaphragm

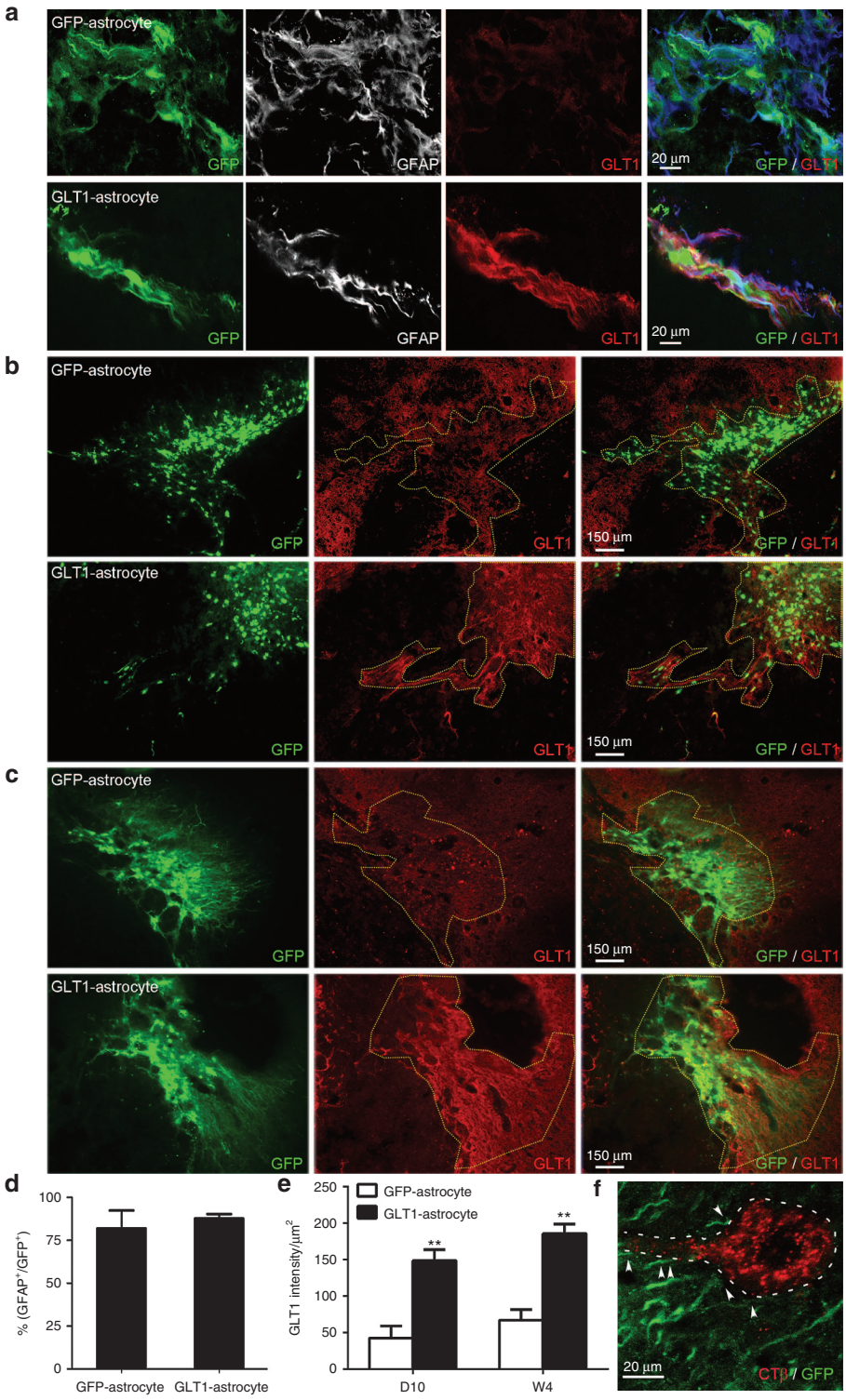

Figure 4 GLT1 overexpression significantly enhances GLT1 protein expression by transplanted astrocytes in the injured cervical spinal cord. We transplanted (i) rat GRP-derived astrocytes transduced prior to transplantation with AAV8-GFA2 control vector (GFP-astrocyte) or (ii) rat GRP-derived astrocytes transduced prior to transplantation with AAV8-GFA2-GLT1 vector (GLT1-astrocyte) into the injured spinal cord immediately following C4 hemicontusion SCI. Both cell groups were also transduced with lentiviral vector for labeling of all cells (regardless of their phenotype) with a GFP reporter. (**a**) At day 10 after injection, the vast majority of transplant-derived GFP$^+$ cells in both groups expressed GFAP (quantification in **d**). At both (**b**) D10 and (**c**) W5 after transplantation into the injured spinal cord, the control transplants expressed very low levels of GLT1 protein, while the overexpressing transplants expressed greatly increased levels of GLT1 protein (area of transplant-derived GFP$^+$ cells marked by dotted line). GLT1 protein signal intensity was quantified within the regions of surviving GFP$^+$ transplant-derived cells at both (**e**) D10 and W4 after transplantation/injury. (**f**) Transplant-derived cells spatially localized around PMNs, which were retrogradely labeled from the ipsilateral hemidiaphragm with the tracer, CTβ. Results were expressed as means ± SEM. *$P < 0.05$, **$P < 0.01$, $n = 5–7$ per group.

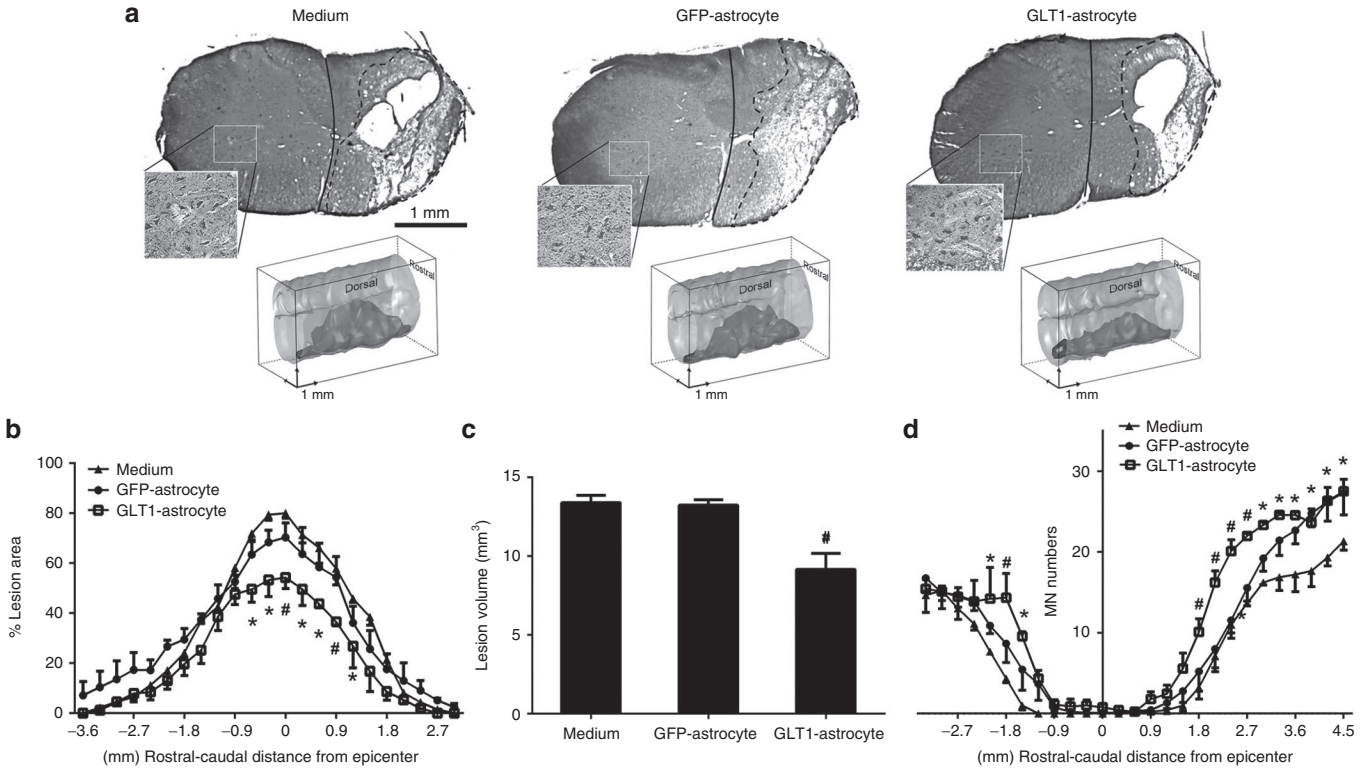

Figure 5 GLT1 overexpressing astrocyte transplants reduce lesion size following cervical contusion SCI. GLT1-overexpressing astrocytes (GLT1-astrocyte), control astrocytes (GFP-astrocytes) or medium-only control were transplanted immediately following C4 hemicontusion SCI. (**a**) Representative images of Cresyl-violet staining and three dimensional reconstruction illustrate the lesion epicenter and entire lesion extent, respectively, in the groups at 10 days after injury. (**b**) Lesion size and (**c**) total lesion volume were reduced in the GLT1-astrocyte group compared to the two control groups. (**d**) Large motor neuron populations in the ventral horn ipsilateral to the contusion site were identified (inset in **a** shows contralateral ventral horn as an example of motor neuron labeling), quantified, and plotted at multiple distances from the epicenter. Results were expressed as means ± SEM. *$P < 0.05$, GLT1-astrocyte group *versus* medium control group. $^{\#}P < 0.05$, GLT1-astrocyte group versus both control groups. $n = 6$ rats per group.

neuromuscular junction (NMJ), the synapse which is critical for functional PMN-diaphragm connectivity. To examine pathological alterations at the diaphragm NMJ, we examined hemidiaphragm muscle ipsilateral to the contusion. We quantified the percentage of intact NMJs in the animals from the three injection groups at 5 weeks after injury/transplantation (**Figure 6a**).[20–22] For analysis, the hemidiaphragm was divided into three anatomical regions (ventral, medial, and dorsal) (**Figure 6b**), as the rostrocaudal axis of the PMN pool within the cervical spinal cord topographically maps onto the ventro-dorsal axis of the diaphragm.[23] While areas of muscle denervation were observed in all three regions, the most pronounced denervation occurred in the dorsal diaphragm, as this is primarily innervated by PMNs located in the C4/C5 spinal cord (*i.e.*, the location of contusion). At the ventral and medial regions of the diaphragm, there were no differences in the percentage of intact NMJs amongst the groups (**Figure 6c**), which coincides with the lack of a protective effect (on lesion size) of GLT1 overexpressing transplants at more distant locations from the lesion epicenter. However, GLT1 overexpressing transplants significantly increased the percentage of intact junctions in the dorsal diaphragm compared to medium-only control by two- to threefold (**Figure 6c**), with the control transplants showing a nonsignificant intermediate phenotype that may be due to the protective effects of GRP-astrocytes independent of GLT1.[24] No differences amongst groups were noted in the percentage of multiply-innervated NMJs at any subregion of the hemidiaphragm (**Figure 6d**), suggesting that sprouting from intact fibers and reinnervation of denervated NMJs was not responsible for the beneficial effects of GLT1 overexpressing transplants.

GLT1 overexpressing astrocyte transplants preserve diaphragm function following cervical contusion SCI

To determine the efficacy of preserving PMN-diaphragm innervation with respect to respiratory impairment, we characterized the *in vivo* functional effects of GLT1 overexpressing transplants on diaphragmatic function. We conducted two types of electrophysiological analysis of functional innervation of the ipsilateral hemidiaphragm by PMNs: spontaneous EMG recordings and phrenic nerve conduction studies.

We conducted recording of spontaneous EMG activity, which is indicative of PMN activation of the muscle, at day 10 after injury/transplantation (**Figure 7a**). For this analysis, needle electrodes were used to specifically record from the same subregions of the hemidiaphragm muscle tested for NMJ morphology. All groups showed reduced amplitude in EMG signal associated with muscle contraction compared to uninjured animals.[25] Integrated EMG analysis of this recording shows that the GLT1 overexpressing transplants significantly increased EMG amplitude in

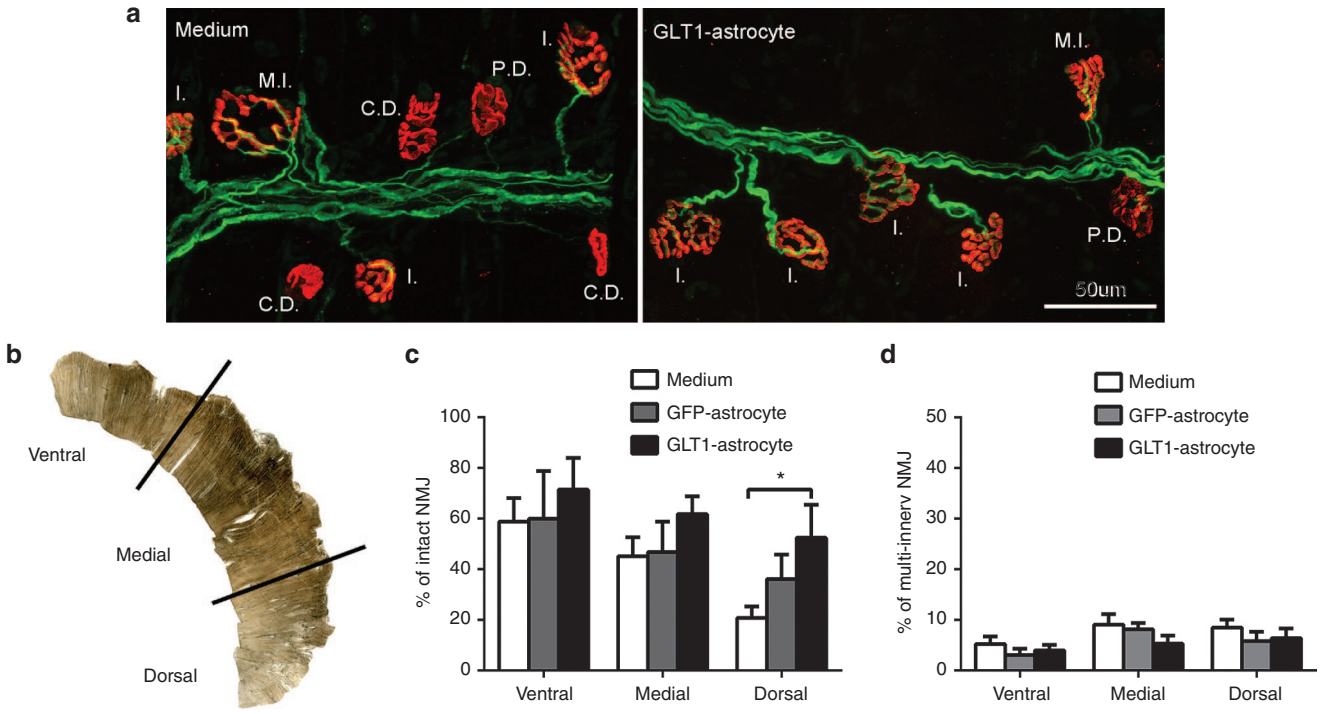

Figure 6 GLT1 overexpressing astrocyte transplants preserve diaphragm innervation by phrenic motor neurons following cervical contusion SCI. Diaphragm NMJs ipsilateral to the hemicontusion were assessed via labeling with Alexa-647 conjugated α-bungarotoxin (red), SMI-312R (green) and SV2-s (green). Areas of muscle denervation were observed in all three groups. (**a**) Representative confocal images are shown for the medium control and GLT1-astrocyte groups. Reduced denervation can be observed in the GLT1-astrocyte muscle compared to the medium control group. Individual NMJs were characterized as: intact (I.); completely denervated (C.D.); partially denervated (P.D.); multiply innervated (M.I.). (**b**) For analysis, the hemidiaphragm was divided into three anatomical subregions (ventral, medial, and dorsal). (**c**) GLT1 overexpressing transplants significantly increased the percentage of intact junctions in the dorsal diaphragm compared to medium-only control by two- to threefold. (**d**) No differences amongst groups were noted in the percentage of multiply-innervated NMJs at any subregion of the hemidiaphragm. Results were expressed as means ± SEM. *$P < 0.05$, GLT1-astrocyte group versus medium control group. $n = 5–7$ rats per group.

the medial and dorsal regions of the hemidiaphragm compared to control groups (**Figure 7b**), again matching the anatomically specific spinal cord and NMJ histological results. However, no protective effects of overexpressing transplants were observed at the ventral region, and the control cell transplants had no significant effects compared to medium injection at all muscle locations. Overexpressing transplants also increased burst duration in the dorsal muscle region (**Figure 7c**); however, no differences amongst any of the groups were noted for burst frequency (**Figure 7d**).

Following supramaximal phrenic nerve stimulus, we obtained compound muscle action potentials (CMAPs) recordings from the ipsilateral hemidiaphragm using a surface electrode (**Figure 7e**). In all treatment groups, peak CMAP amplitude was significantly reduced compared to uninjured laminectomy only animals, whose CMAP amplitudes are ~8 mV.[25] However, CMAP amplitudes in the GLT1 overexpressing transplant group were significantly increased compared to the other two groups at weeks 1, 3, and 4 after injury (**Figure 7f**). With the use of the surface electrode, we are recording from the entire hemidiaphragm (or at least a significant portion of the muscle), yet we still observed this significant protective effect on overall muscle function, despite the fact that transplants only reduced central degeneration very near to the injury site and correspondingly preserved morphological innervation only in the dorsal diaphragm. We found no differences amongst groups in forelimb motor performance using grip strength testing (**Figure 7g**).

Glial scar reduction was not responsible for effects of GLT1 overexpressing transplants

To identify whether cell transplantation groups altered astroglial scar formation, we performed *in vivo* scar border formation analysis at both 10 days and 4 weeks after injury/injection (**Figure 8a**). At 4 weeks after injury (but not at 10 days after injury), we observed reduced glial scar formation with both transplant groups compared to medium-only control (**Figure 8b**). However, we found no differences between the two transplant groups at this 4 week time point (**Figure 8b**).

DISCUSSION

Our findings show that anatomically targeted intraspinal transplantation of glial progenitor-derived astrocytes engineered to overexpress GLT1 into the ventral horn therapeutically reduces spinal cord lesion size, diaphragm NMJ denervation by PMNs, and diaphragmatic respiratory dysfunction following cervical hemicontusion SCI. Collectively, these data demonstrate that neural stem/progenitor transplantation-based replacement of GLT1 is a promising therapeutic approach for SCI.

Astrocytes have traditionally been viewed in a negative light following CNS trauma because of their roles in glial scarring,

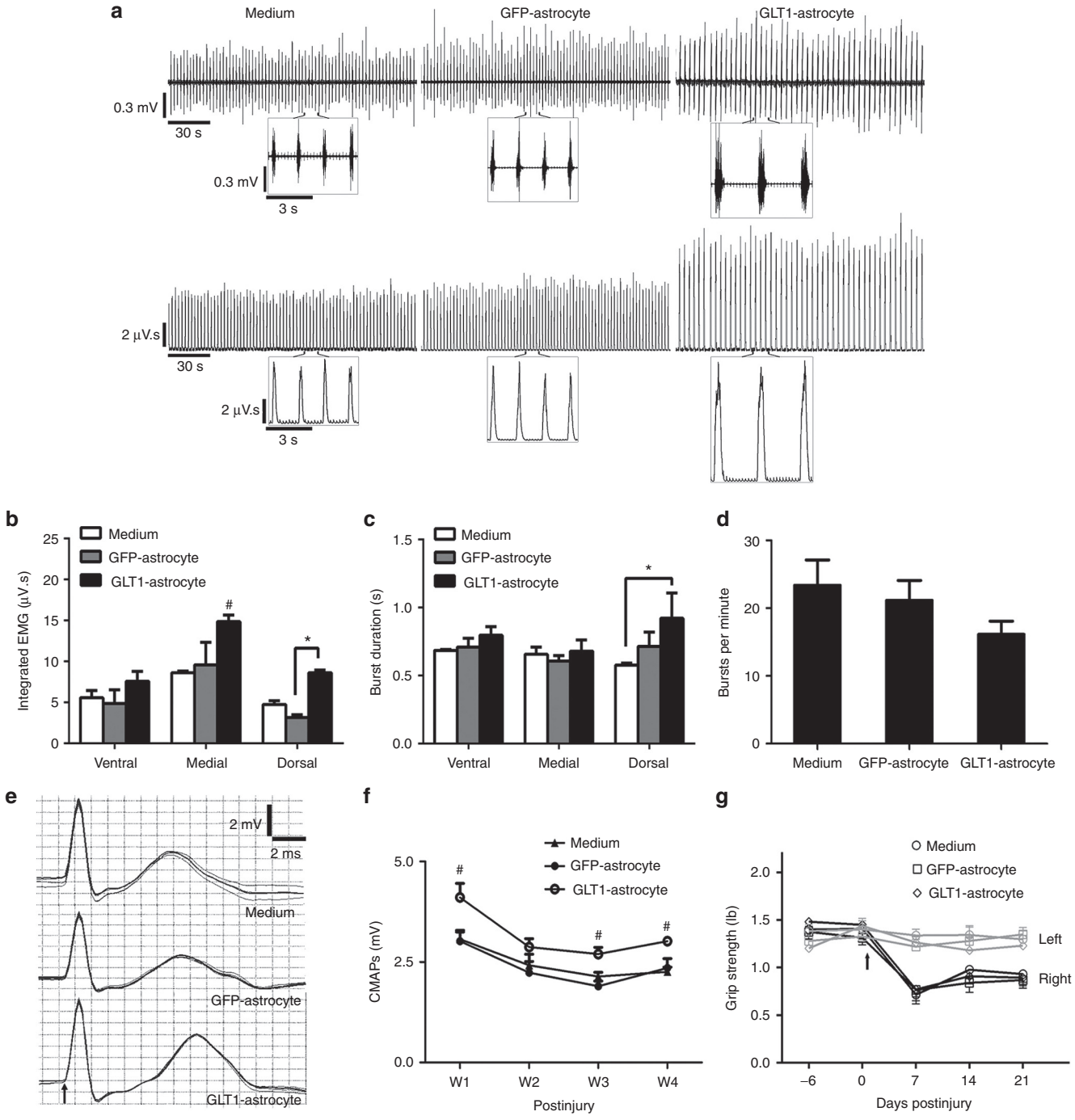

Figure 7 GLT1 overexpressing astrocyte transplants preserve diaphragm function following cervical contusion SCI. (**a**) At D10 after injury/transplantation, spontaneous diaphragm electromyography (EMG) recordings were performed and are shown as raw voltage output (upper panels) and integrated signals (lower panels), and the individual breaths are shown in **a** (inset). (**b**) Integrated EMG amplitude, (**c**) inspiratory burst duration, and (**d**) inspiratory bursts per minute in the ipsilateral hemidiaphragm were averaged over a 2 minute period. (**e**) Diaphragm compound muscle action potentials (CMAPs) obtained following supramaximal stimulation (arrow in **e** denotes time of stimulation) were recorded in the ipsilateral hemidiaphragm. (**f**) Compared to the two control groups, peak CMAP amplitudes were significantly larger in the GLT1-astrocyte group at W1, W3, and W4 after injury/transplantation. No differences were observed amongst groups in forelimb motor performance using grip strength testing (**g**). Results were expressed as means ± SEM. $^{*}P < 0.05$, GLT1-astrocyte group versus ether medium control group or GFP-astrocyte control group only. $^{\#}P < 0.05$, GLT1-astrocyte group versus both control groups. $n = 6$ rats per group for CMAP recordings; $n = 3$ rats per group for EMG recordings.

proinflammatory cytokine release and other processes. However, their crucial neuroprotective/homeostatic roles, including GLT1-mediated glutamate uptake, have not been extensively targeted therapeutically in SCI models, despite obvious therapeutic implications.[9] A number of studies have shown that glutamate-mediated excitotoxic cell death/injury plays a central part in secondary degeneration of various CNS cell types in the hours-to-days post-SCI. Exogenous parenchymal administration of glutamate to

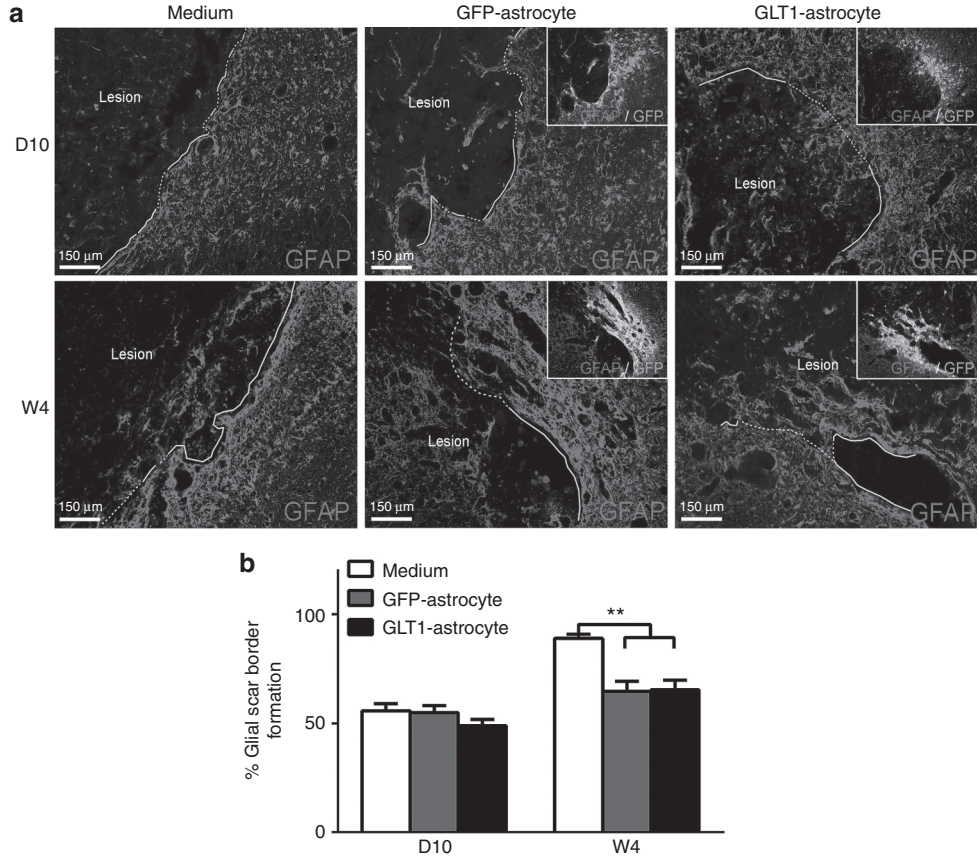

Figure 8 Glial scar reduction is not responsible for the therapeutic effects of GLT1 overexpressing transplants. (**a**) At 10 days (D10) and 4 weeks (W4) after injury, immunostaining with anti-GFAP antibody was performed. In cell transplantation groups, the border containing GFP$^+$ transplant-derived cells was analyzed (**a**, inset). Astroglial scar border is highlighted as yellow solid line. At W4 after injury (but not at D10 after injury), we observed (**b**) reduced glial scar formation with both control and GLT1 overexpressing transplant groups compared to medium-only control. However, we found no differences in the degree of reduced scar formation between the two transplant groups at this W4 time point (**b**). Results were expressed as means ± SEM. $^{**}P < 0.01$, $n = 6$ rats per group for analysis of scar formation.

uninjured spinal cord results in tissue and function loss similar to SCI.[26] While large increases in glutamate can occur shortly after SCI, elevation can also persist depending on injury severity.[27] In addition to focal increases, levels can also rise in regions removed from the lesion site, possibly via a spreading mechanism involving activated glia.[28] Early gray matter loss is likely mediated by NMDA receptors, while delayed loss of neurons and oligodendrocytes, as well as axonal and myelin injury, is thought to be predominantly mediated via AMPA over-activation.[7] In the context of SCI-induced respiratory dysfunction, we previously reported that following cervical contusion SCI there is significantly compromised astrocyte GLT1 expression in cervical ventral horn. Importantly, this GLT1 loss occurs at early time points after injury within the temporal window of PMN degeneration, providing a therapeutic target for PMN preservation.

Targeting lost and/or dysfunctional astrocytes via cell transplantation is a promising, yet understudied, therapeutic approach for SCI. Transplants can be anatomically delivered specifically to cervical spinal cord ventral horn to target the location of PMNs for neuroprotection.[13] Alternative strategies such as gene therapy only target one (or at most a few) specific gene(s), while astrocyte transplantation can participate in the restoration of a host of astrocyte functions. Transplantation also provides for long-term astrocyte integration and therapeutic replacement. For example, the lasting nature of dysregulation of extracellular glutamate homeostasis after SCI[15] calls for longer-term maintenance of therapeutic effects, both with respect to early PMN loss and other outcomes of SCI associated with more persistent pathophysiology of glutamate signaling such as neuronal hyperexcitability.[28,29]

The use of glial progenitor cells is particularly promising for achieving targeted astrocyte replacement. GRPs are lineage-restricted neural progenitor cells isolated from developing and adult CNS based on expression of the cell surface marker, A_2B_5.[14] GRPs can be expanded in culture and differentiated into only astrocytes and oligodendrocytes, but not neurons. Following intraspinal transplantation into models of SCI and amyotrophic lateral sclerosis (ALS), we and others previously showed that rodent- and human-derived GRPs robustly survive in the diseased spinal cord, migrate extensively from focal injection sites, efficiently differentiate into astrocytes, acquire mature astrocyte morphology, and do not display uncontrolled proliferation or tumor formation.[13] In addition, we were able to use GRP transplantation to successful replace lost astrocyte GLT1 in cervical spinal cord ventral horn in the transgenic rat SOD1^{G93A} model of ALS, which resulted in therapeutic protection of PMN-diaphragm function and a delay in disease-induced animal death.[13] Combined with our present

results, these studies demonstrate that mechanistically targeting important astrocyte-specific functions represents a powerful approach for treating CNS diseases associated with extracellular glutamate dysregulation.

Despite the efficaciousness of our current approach, these findings appear to contradict our earlier work. In a previous study,[10] we reported that AAV-based astrocyte-specific elevation of GLT1 expression in endogenous astrocytes of the cervical ventral horn in this same C4 hemicontusion model worsened secondary loss of PMNs, diaphragm denervation and diaphragm dysfunction. In that study, we showed that increasing GLT1 expression in endogenous reactive astrocytes post-SCI compromised their protective glial scar-forming ability both *in vitro* and *in vivo*. Given the critical role played by the astroglial scar after SCI in minimizing expansion of the lesion site, these findings provide caution for strategies aimed at modulating the properties of this important astrocyte population. Based on these data, we took a different approach in the current study. We now find that providing an exogenous glial progenitor-derived source of astrocytes allows for efficient replacement of GLT1 in the injured cervical spinal cord, which resulted in significant protection of respiratory neural circuitry and preservation of diaphragm function. Taken together, our findings suggest that enhancing astrocyte GLT1 expression following SCI is an efficacious way to reduce secondary degeneration and preserve function. This contention is supported by another previous study in which we showed decreased functional recovery and increased ventral horn neuron loss in GLT1 heterozygous mice following thoracic crush SCI.[15] However, this strategy of GLT1 elevation will likely not be beneficial when endogenous astrocytes are targeted at early time points after spinal cord trauma. Increasing GLT1 expression in endogenous populations is likely still a useful approach when more delayed events are targeted, possibly after the formation of the astroglial scar and the period of secondary degeneration have ended.

A number of studies have demonstrated the therapeutic potential of GRP transplantation into a variety of SCI models. Most of this previous work was focused on the capacity of GRPs and GRP-derived astrocytes to induce host axonal regrowth in the injured spinal cord.[30–32] Our study represents a different approach in which we mechanistically targeted a central homeostatic function of astrocytes. We found that, similar to endogenous astrocytes, GRP transplant-derived astrocytes do not express high levels of GLT1 in the injured spinal cord, while expression levels in transplant-derived cells are greater following injection into intact spinal cord. Even though these astrocytes are derived from an exogenous source, they still appear to respond to signals generated at the injury site in a similar fashion as the host population. These findings demonstrate the important concept that targeted and efficient differentiation of GRP transplants into GFAP-expressing cells does not necessarily result in the generation of functionally mature astrocytes. Instead, specific astrocytes functions need to be assessed following engraftment to best understand their maturation and, importantly, their therapeutic contribution. To address the limited expression of GLT1, we engineered GRPs to constitutively overexpress the transporter *in vitro* prior to transplantation using an AAV vector that drives expression only in GFAP-positive astrocytes. We observed therapeutic efficacy in our battery of histological and functional assays only with the GLT1-overexpressing transplants, suggesting that astrocyte replacement alone without GLT1 expression is not sufficient for promoting significant PMN neuroprotection in this SCI model. We did observe an intermediate protective phenotype with unmodified GRP transplants for preserving diaphragm NMJ innervation. Previous work has shown that GRP transplants can exert some degree of neuroprotection, and GRPs and GRP-derived astrocytes express measurable levels of potentially beneficial molecules such as neurotrophic factors.[13] Therefore, it is likely that unmodified GRP-derived astrocytes do provide a limited degree of neuroprotection in SCI, but modification of these cells is necessary to boost their therapeutic potential.

The *in vivo* expression of GLT1 by graft-derived astrocytes has not been tested following transplantation into injured spinal cord. As successful targeting of PMN protection following cervical SCI critically depends on the integration and functional maturation of transplanted astrocytes,[11] we characterized the survival, anatomical localization, differentiation and, importantly, GLT1 expression by transplanted GRPs and GRP-derived astrocytes following intraspinal injection into both the intact/uninjured and injured cervical spinal cord. Our results showed that, similar to endogenous astrocytes following contusion SCI,[15] transplant-derived astrocytes have reduced propensity for GLT1 expression and function, which has important relevance for their therapeutic potential in SCI and other CNS diseases associated with GLT1 pathophysiology.

We[13,33–36] and others[37,38] have extensively characterized the *in vivo* properties of transplanted rodent glial progenitors in both the intact nervous system and in CNS disease models. In addition, more clinically relevant populations of human glial progenitors have been isolated, characterized, and transplanted into the injured spinal cord. Again, these studies with human cells were primarily focused on the ability of transplants to induce host axonal plasticity. With an eye towards developing a viable therapeutic approach for SCI patients, it will be important to test our current GLT1-targeted strategy in the cervical contusion model using human GRPs and other relevant sources such as human iPS cell[39] -derived glial progenitors and astrocytes. In addition to protection of respiratory neural circuitry, restoring GLT1 function likely has therapeutic potential for targeting other outcomes following SCI associated with GLT1 pathophysiology, including chronic neuropathic pain that is accompanied by persistent downregulation of GLT1 in superficial dorsal horn.

We employed anatomically specific delivery of transplants to the ventral horn at midcervical levels for therapeutically targeting PMN protection. This approach is crucial for developing a region-specific treatment that avoids unwanted side effects. For example, targeting glutamate receptor over-activation (*e.g.*, AMPA and NMDA antagonists) for blocking glutamate-mediated excitotoxicity following SCI has diffuse and nonspecific effects in CNS, PNS and potentially other tissues, as well as only a short duration of intervention.[40] In this way, we aimed to develop a relevant therapeutic strategy for humans suffering from respiratory compromise following cervical SCI.

We found that all animals, regardless of transplant group, exhibited similar ipsilateral grip strength performance,

demonstrating the consistency of our injury paradigm. The lack of differences amongst groups also shows that GLT1-overexpressing transplants exerted a specific effect on PMNs and not forelimb motor neurons, which is not unexpected given that cells were transplanted close to the C4 level (the location of the PMNs pool) while distal forelimb motor neuron pools are located at more caudal spinal cord levels (where cells were not transplanted).

In this study, we focused on assessing preservation of PMNs and diaphragm innervation. In our previous work,[10] we found that manipulating GLT1 expression levels using AAV8 delivery affected the survival of both large α motor neurons and smaller neuronal populations of the cervical spinal cord, demonstrating that GLT1 function does not have selective effects on motor neurons. It is likely that some of these smaller neurons were respiratory interneurons; however, we did not specifically identify them using an anatomical approach such as trans-synaptic labeling from the diaphragm or VRG. We realize that other respiratory neural mechanisms may have also contributed to our observed functional effects, including protection of respiratory interneurons of the cervical spinal cord, preservation of descending bulbospinal innervation from the ventral respiratory group (VRG) and possibly even regrowth/regeneration and/or sprouting of bulbospinal axons originating from the ipsilateral and/or contralateral VRG. Ongoing work is aimed at evaluating the contribution of these neural substrates to the effects of our intervention.

In this study, we have analyzed peripheral sprouting of spared PMN axons at the diaphragm NMJ, but we did not observe any differences amongst transplant groups, suggesting that beneficial effects were most likely due to central mechanisms occurring in the cervical spinal cord. We only conducted NMJ analysis in ipsilateral hemidiaphragm because in our previously published work we did not observe denervation or sprouting in contralateral hemidiaphragm after cervical hemicontusion SCI.[25]

We observed reduced glial scar formation with both transplant groups compared to medium-only control, demonstrating that glial transplantation can modulate endogenous scar formation following SCI. However, we found no differences in scar formation between the two transplant groups. Because we do find a beneficial effect on neuroprotection, preservation of diaphragm NMJ innervation and diaphragm function (with EMG and CMAP analyses) only with GLT1 overexpressing transplanted cells (and not with control transplants), these data suggest that modulation of scar formation (and consequent effects on axonal growth) is likely not the mechanism responsible for the therapeutic effects of GLT1 overexpressing transplants.

While a growing literature exists on respiratory dysfunction in animal models of SCI,[1,2] relatively few studies have examined cellular mechanisms involved in protection of this vital neural circuitry, and little work has been conducted to test therapies for targeting cervical spinal cord-related functional outcome measures such as breathing. This urgently calls for development of interventions targeting respiratory protection after cervical SCI to address this debilitating patient problem. Although use of thoracic injury models has predominated, cervical SCI animal models have recently been developed,[41–43] including our well-characterized unilateral midcervical hemicontusion SCI model.[25] This hemicontusion paradigm provides a number of key advantages. The contusion is one of the most widely used SCI paradigms and closely models the majority of human SCI cases, providing clinical relevance to therapeutic findings. Significant cell and function loss results from secondary degeneration involving glutamate dysregulation.[44] Importantly, we have also optimized a number of assays for measuring human SCI-relevant histopathological and functional outcomes associated with PMN-diaphragm function in this injury.[25] Using this powerful model system, we have demonstrated that an astrocyte mechanism-specific approach results in significant protection of a respiratory neural circuit that plays a central role in SCI patient outcome.

MATERIALS AND METHODS

Animals

BAC-GLT1-eGFP mice: Transgenic bacterial artificial chromosome (BAC)-GLT1-enhanced green fluorescent protein (eGFP) transgenic promoter reporter mice were previously generated by Regan *et al.*[16] and were a kind gift from Jeffrey Rothstein's laboratory at John Hopkins University. BAC-GLT1-eGFP mice were used to derive cultures of GRPs to examine *in vivo* GLT1 expression by transplant-derived cells following intraspinal injection.

Transplantation into rats: Female Sprague-Dawley rats weighing 250–300 g were purchased from Taconic Farm (Rockville, MD). Rats were divided into two paradigm groups according to the experimental design described below. All animals were housed in a humidity-, temperature-, and light-controlled animal facility with *ad libitum* access to water and food. Experimental procedures were approved by the Thomas Jefferson University institutional animal care and use committee and conducted in compliance with the European Communities Council Directive (2010/63/EU, 86/609/EEC, and 87-848/EEC), the NIH Guide for the care and use of laboratory animals, and the Society for Neuroscience's Policies on the Use of Animals in Neuroscience Research.

Experimental design

BAC-GLT1-eGFP GRP transplantation paradigm: Wild-type Sprague-Dawley rats were subjected to cervical hemicontusion SCI at the C4 level,[10,45] and were then immediately transplanted with either undifferentiated GRPs or GRP-derived astrocytes (*i.e.*, predifferentiated into GFAP+ astrocytes prior to injection). GRPs used for this experiment were derived from BAC-GLT1-eGFP fluorescence reporter mice and transduced with retrovirus-RFP vector. Cells were transplanted into the ventral horn at two locations in all animals: (i) directly into the injury site; (ii) into the contralateral spinal at level C5 (one spinal segment below and contralateral to the injury site). Rats were then euthanized at 2, 14, or 35 days after injury (DPI) (n = 6 per group per time point). For this paradigm, no assessment of functional or histopathological efficacy of transplantation was conducted. These animals were only used to track transplant fate.

Therapeutic efficacy transplantation paradigm: As opposed to a single injection into the lesion site and a single injection at a distant intact site, this paradigm was optimized in an attempt to achieve maximal therapeutic benefit in the unilateral C4 hemicontusion model with respect to obtaining PMN protection and preservation of diaphragm function. Cells were transplanted into the ventral horn at three injection locations ipsilateral to the contusion site (immediately after injury): directly into the lesion epicenter (1.0×10^6 cells), as well as one-half segment rostral and caudal to the epicenter (two injections of 0.5×10^6 cells/each). Three injection groups were compared: (i) GRP basal medium-only control; (ii) GRP-derived astrocytes transduced prior to transplantation with AAV8-GFA2-eGFP control vector; (iii) GRP-derived astrocytes transduced prior to transplantation

with AAV8-GFA2-GLT1 overexpression vector. Both cell groups were also transduced with lentiviral vector for labeling all cells (regardless of their phenotype) with a GFP reporter. For this paradigm, undifferentiated GRPs were not transplanted. Animals were examined for both functional and histopathological outcomes and were then euthanized at 10 or 28 days after injury (n = at least eight per group per time point).

***Glial-restricted precursor (GRP) derivation, culture and differentiation* in vitro.** GRPs were derived from the spinal cord of E13 embryos of BAC-GLT1-eGFP mice or Sprague–Dawley rats, as described previously[46] with slight modifications. Briefly, the spinal cords were isolated from embryos, and the meninges were removed. The spinal cords were dissociated to single-cell suspensions with Neural Tissue Dissociation Kits (Miltenyi Biotec, San Diego, CA). $A_2B_5^+$ GRPs were positively selected with Anti-A_2B_5 MicroBeads using magnetic cell separation technology (Miltenyi Biotec). GRPs were seeded onto poly-L-lysine coated 100 mm dishes and cultured with GRP medium: DMEM/F12 (Life Technologies, Grand Island, NY) + B27 (Life Technologies) + Bovine Serum Albumin (0.1% w/v) + bFGF (10 ng/ml; PeproTech, Rocky Hill, NJ).[14] To induce differentiation into astrocytes, GRPs were cultured in differentiation medium consisting of GRP medium supplemented with 10 ng/ml BMP4 (PeproTech) and lacking the mitogen bFGF. To induce GLT1 up-regulation during *in vitro* differentiation, GRPs/astrocytes were cultured with neuronal-conditioned medium[17] supplemented with 10 ng/ml BMP4.

Virus production and delivery. Two recombinant AAV8 vectors carrying eGFP or GLT1 driven by the Gfa2 promoter were constructed to specifically target expression in astrocytes. The viral vectors were prepared as previously described.[10] Recombinant AAV8 was packaged in HEK293T cells. Approximately 1.5×10^7 cells were seeded into 150 cm dishes in DMEM supplemented with 10% FBS, 1 mmol/l MEM sodium pyruvate, 0.1 mmol/l MEM nonessential amino acids and 0.05% Penicillin-Streptomycin (5,000 units/ml). At 24 hours after cell seeding, medium was changed to culture medium containing only 5% FBS, and cells were transfected with three plasmids: adeno helper plasmid (pFΔ6), AAV helper encoding serotype 8 (pAR8, kindly provided by Miguel Sene Esteves at the University of Massachusetts) and the AAV packaging vector containing the glial fibrillary acidic protein (GFAP) promoter flanked by either the eGFP gene or the human EAAT2 (GLT1a) gene sequence (obtained from Jeffrey Rothstein's laboratory). Plasmids were transfected into HEK293T cells using Polyfect according to the manufacture's specifications (Qiagen, Valencia, CA). Cultures were incubated at 37 °C, 5% CO_2. After 72 hours, cells were harvested and pelleted by centrifugation. The pellet was re-suspended in 10 mmol/l Tris, pH 8.0 and chilled on ice. Cells were lysed by repeated freeze-thaw cycles, followed by treatment with 50 U benzonase (Novagen) and 0.5% sodium deoxycholate for 30 minutes at 37 °C. The lysate was sonicated three times. Virus was then purified by density gradient centrifugation in iodixanol according to the method of Zolotukhin *et al.*[47] Each AAV vector preparation was sterile filtered, and the titer (genomic particles/ml) was determined by quantitative RT-PCR using primers and a probe specific for the WPRE sequence and then diluted with artificial cerebrospinal fluid to 1×10^{13} genomic particles/ml.

Lentiviral vector carrying the green fluorescent protein (GFP) gene was packaged in 293FT cells. 293FT cells were transfected with pCDH-MSCV-MCS-EF1-GFP plasmid (System Biosciences, Mountain View, CA) and three other helper vectors, pLP-1, pLP-2, and pLP/VSVG with Polyfect (Qiagen). Supernatant was collected 72 hours later, and lentiviral vector was concentrated with PEG-it Virus Precipitation Solution (System Biosciences) and resuspended with PBS to the final titer of 1×10^8 infectious units/ml.

Retroviral vector carrying the red fluorescent protein (RFP) gene was packaged in 293FT cells. 293FT cells were transfected with plasmid pMXs-mRFP1 (Addgene, Cambridge, MA) and helper plasmid pCL-Eco.[48] Supernatant was collected 72 hours later, and the retroviral vector was concentrated with PEG-it Virus Precipitation Solution (System Biosciences) and resuspended with PBS to the final titer of 1×10^8 infectious units/ml.

Cell preparation for transplantation. For tracing the transplanted cells *in vivo,* cells were labeled with RFP or GFP gene using retroviral or lentiviral vector, respectively, 3 days before transplantation. For BAC-GLT1-eGFP GRP transplantation, cells were transduced with retrovirus-RFP. For rat GRP-derived astrocyte transplantation, GRPs were induced towards astrocyte differentiation for 3 days and infected with AAV-eGFP or AAV-GLT1 vector, at an MOI (Multiplicity of Infection) of 5×10^4 vector genomes per cell. The differentiated rat cells were transduced with lentivirus-GFP 1 day later. On the day of transplantation, cells were treated with StemPro Accutase (Life Technologies) or trypsin (Life Technologies). The cells were washed with fresh medium two times. Cell viability was assessed using the trypan blue assay and was always found to be greater than 75%. The final cell concentration was adjusted to 1.5×10^8 cells/ml for transplantation.

Cervical contusion SCI and cell transplantation. All rats throughout this study were immune suppressed by subcutaneous administration of cyclosporine A (10 mg/kg; Sandoz Pharmaceuticals, East Hanover, NJ), daily beginning 7 days before surgery and continuously until euthanasia.

Cervical hemicontusion SCI was performed on rats. Rats were anesthetized with ketamine (100 mg/kg), xylazine (5 mg/kg) and acepromazine (2 mg/kg). The cervical dorsal skin and underlying muscles were incised. The paravertebral muscles overlying C3-C4 were removed. Following unilateral laminectomy on the right side at C4 levels, rats were subjected to a C4 hemicontusion SCI with the Infinite Horizon impactor (Precision Systems and Instrumentation, Lexington, KY) using a 1.5 mm tip at a force of 395 kDynes. These injury paradigms are based on our previously published rat model that result in robust PhMN degeneration and chronic diaphragm dysfunction.[18,25]

In our previous work,[13,49] we varied the number of cells injected per site, as well as the volume injected per site, to determine the optimal paradigm for delivering a therapeutically beneficial numbers of cells without causing unwanted injection-induced damage. We therefore based our current injection paradigm on these findings. Following injury, two to three injections, each containing 2 µl of cells (1.5×10^8 cells/ml), were administered into the spinal cord ventral horn, at a depth of 1.5 mm below the dorsal cord surface to specifically target ventral horn PMNs[10,13] at levels C3, C4, and C5 using a Hamilton gas-tight syringe mounted onto an electronic UMP3 micropump (World Precision International, Sarasota, FL).[50] As shown in **Figure 2a**, the sites of injections were targeted along the rostral-caudal axis with a virtual line connecting the points of dorsal root entry and in the lateral axis corresponding to the middle of each spinal segment (C4, C5, or C6). Each injection was delivered at a constant rate over 5 minutes. After surgical procedures, overlying muscles were closed in layers with sterile 4-0 silk sutures, and the skin incision was closed using wound clips. Animals were allowed to recover on a circulating warm water heating pad until awake and then returned to their home cages. They were monitored daily until euthanasia, and measures were taken to avoid dehydration and to minimize any pain or discomfort. No signs of bladder or bowel dysfunction were ever detected following injury.

Retrograde anatomical tracing of phrenic motor neurons. Two weeks before sacrificing the rats, CTβ conjugated to Alexa555 (Life Technologies) was injected unilaterally into the intrapleural space of the ipsilateral hemidiaphragm muscle.[10,25] This procedure allowed for the specific labeling of PMNs innervating the diaphragm through retrograde transport of CTβ fluorescent tracer. Following laparotomy under anesthesia, 15 µl of CTβ (0.2% solution in distilled water) was intrapleurally delivered through the diaphragm (3 injections of 5 µl each) using a 20 µl Hamilton syringe with an attached 33-gauge needle. Abdominal muscles were then sutured with 4-0 sutures, and skin was closed with wound clips.

Tissue processing for histology. At the time of euthanasia, animals were anesthetized, and diaphragm muscle and phrenic nerves were freshly removed prior to paraformaldehyde perfusion and then further processed for neuromuscular junction (NMJ) labeling. Animals were transcardially

perfused with 0.9% saline, followed by 4% paraformaldehyde infusion. Spinal cords were harvested, then cryoprotected in 30% sucrose for 3 days and embedded in freezing medium. Spinal cord tissue blocks were cut serially in the transverse plane at a thickness of 30 μm. Sections were collected on glass slides and stored at −20 °C until analysis. Spinal cord sections were thawed, allowed to dry for 1 hour at room temperature, and stained with 0.5% Cresyl violet acetate according to standard procedure.[25] For RFP/eGFP cell counting, frozen spinal cord sections were air-dried, washed and cover-slipped with fluorescent-compatible mounting medium (ProLong Gold, Life Technologies).

Neuromuscular junction (NMJ) analysis. Fresh hemidiaphragm muscle was dissected from each animal for whole-mount immunohistochemistry, as described previously.[10,20] Animals that did not receive CTβ injections were used for this study to avoid overlap of Alexa555-conjugated CTβ with the rhodamine-conjugated α-bungarotoxin used to label the nicotinic acetylcholine receptors. Muscle was stretched, pinned down to Sylgard medium (Fisher Scientific, Pittsburgh, PA), and extensively cleaned to remove any connective tissue to allow for antibody penetration. Motor axons and their terminals were labeled with SMI-312R (Covance, Princeton, NJ) and SV2-s (DSHB, Iowa City, IA), respectively, and both primary antibodies were detected with FITC anti-mouse IgG secondary (Jackson ImmunoResearch Laboratories, West Grove, PA). Postsynaptic acetylcholine receptors were labeled with rhodamine-conjugated α-bungarotoxin (Life Technologies). Labeled muscles were analyzed for total numbers of NMJs and intact, denervated and multiply-innervated NMJs. Whole-mounted diaphragms were imaged on a FluoView FV1000 confocal microscope (Olympus, Center Valley, PA). We only conducted NMJ analysis in ipsilateral hemidiaphragm because in our previously published work we did not observe denervation or sprouting in contralateral hemidiaphragm after cervical hemicontusion SCI.[25]

Immunohistochemistry. Frozen spinal cord sections were air-dried, washed, permeabilized with 0.4% Triton X-100 in PBS for 5 minutes at room temperature, and then incubated in blocking solution (PBS containing 10% normal goat serum and 0.4% Triton X-100) for 1 hour at room temperature. Sections were labeled overnight at 4 °C with the primary antibodies in blocking solution. Sections were washed three times with PBS (5 minutes per wash) and incubated with secondary antibodies in blocking solution for 1 hour at room temperature. After washing twice with PBS (10 minutes per wash), sections were cover-slipped. A number of primary antibodies were used. Rat anti-M2 antibody (DSHB, Iowa City, IA; 1:200) was used to identify transplanted mouse-derived cells in rat tissue. Mouse anti-GFAP (EMD Millipore, Billerica, MA; 1:200) and rabbit anti-GFAP (Dako North America, Carpinteria, CA; 1:200) were used to label astrocytes. Rabbit anti-GLT1 (1:800) and mouse anti-GLT1 (1:200) were used to label GLT1 protein (both were provided by Jeffrey Rothstein's laboratory).[13] Mouse anti-A_2B_5 (Millipore; 1:50) labeled glial progenitor cells. Secondary antibodies included: Alexa Fluor 488 goat-anti-mouse IgG, Alexa Fluor 488 goat-anti-rabbit IgG, Alexa Fluor 594 goat-anti-mouse IgG, Alexa Fluor 594 goat-anti-rabbit IgG, Alexa Fluor 647 goat-anti-mouse IgG, Alexa Fluor 647 goat-anti-rabbit IgG, Alexa Fluor 594 goat-anti-rat IgG. All secondary antibodies were purchased from Jackson ImmunoResearch Laboratories (West Grove, PA) and diluted at 1:200 to recognize the matched primary antibody.

Analysis of BAC-GLT1-eGFP GRP transplants. At 2, 14, or 35 days after injury/transplantation, rats were euthanized for quantification of GLT1 expression (using the BAC-GLT1-eGFP reporter) by RFP-labeled transplant-derived cells in both the intact and injured spinal cord ventral horn. $eGFP^+$ and RFP^+ cells were identified in the ventral horn using ImageJ software, and the percentage of RFP^+ cells (representing any transplant-derived cell) that coexpressed eGFP was quantified.

Quantification of* in vitro *cultured cell differentiation and GLT1 expression. The proportions of $GFAP^+$ astrocytes and $GLT1^+$ cells were expressed as a percentage of the total number of cultured cells (labeled by DAPI). In order to quantify double-labeling of DAPI with GFAP and GLT1, images were taken at 10× magnification and analyzed using ImageJ software. In each image, cells with a $DAPI^+$ nucleus were assessed for expression GFAP or GLT1. To quantify GLT1 fluorescence signal intensity, integrated intensities were measured in ImageJ and calculated to be the GLT1 integrated intensity minus the background integrated intensity. All GLT1 images were acquired using the same exposure settings.

Quantification of GLT1 expression by transplant-derived cells. To quantify GLT1 fluorescence signal in the ventral horn, integrated intensities were measured in ImageJ specifically in the location of GFP^+ transplant-derived cells in both the control and GLT1 overexpressing transplant groups. GLT1 intensity was calculated to be the GLT1 integrated intensity minus the background integrated intensity of the ventral horn. All GLT1 images were acquired using the same exposure settings.

Quantification of* in vivo *astroglial scar border formation. At 10 days and 4 weeks after injury, following immunostaining with mouse anti-GFAP antibody, three to four images per animal (at locations surrounding the injury epicenter) were obtained at 5× magnification. $GFAP^+$ astroglial processes immediately adjacent to the lesion, oriented parallel to the border of lesion (at day 10), and intertwined and overlapped extensively (at 4 weeks), were regarded as the border of astroglial scar. Quantification results are shown as the percentage of astroglial scar border length compared to the length of total lesion border.

Lesion and motor neuron imaging and quantification. Images were acquired with a Zeiss Imager M2 upright microscope and analyzed with ImageJ software. Lesion size was quantified in Cresyl violet stained sections.[10,25] Specifically, lesion area was determined in every 10th section by tracing both the total area of the hemispinal cord ipsilateral to the contusion site and the actual lesion area. Lesion was defined as areas including both lost tissue (cystic cavity formation) and surrounding damaged tissue in which the normal anatomical structure of the spinal cord was lost. The lesion epicenter was defined as the section with the largest percent lesioned tissue (relative to total tissue area in the same section). Ventral horn motor neurons were outlined in these same Cresyl violet stained sections, and the number of motor neuron cell bodies was quantified in a blind manner. α motor neurons with a clearly identifiable nucleus and a cell soma greater than 200 μm^2 (ref. [49]) were counted.

Functional glutamate uptake assay. GRPs were cultured in differentiation medium consisting of GRP basal medium supplemented with 10 ng/ml BMP4 and lacking the mitogen bFGF[30] for 2 days and then transduced with AAV8-Gfa2-eGFP or AAV8-Gfa2-GLT1. Glutamate uptake activity of GRP-derived astrocytes was measured 6 days after transduction, as previously described[10] with slight modification. Briefly, cells were washed and preincubated with either a sodium- or choline-containing uptake buffer (in mmol/l: Tris, 5; HEPES, 10; NaCl or choline chloride, 140; KCl, 2.5; $CaCl_2$, 1.2; $MgCl_2$, 1.2; K_2HPO_4, 1.2; glucose, 10) for 20 minutes at 37 °C; and in DHK treatment groups, 100 μmol/l of DHK was added to inhibit GLT1. The uptake buffer was then replaced with fresh uptake buffer containing 20 nmol/l ^{3}H-glutamate (49 Ci/mmol; PerkinElmer, CA) and 2 μmol/l unlabeled glutamate. The cells were incubated for 5 minutes at 37 °C. The reaction was terminated by washing cells three times with ice-cold uptake buffer containing 2 mmol/l unlabeled glutamate, followed by immediate lysis in ice-cold 0.1 N NaOH. Cell extracts were then measured with a liquid scintillation counter (Beckman Instruments, Fullerton, CA). The protein content in each well was measured using the Bradford protein assay (Bio-Rad, Hercules, CA).

Diaphragm CMAPs. Rats were anesthetized in the same manner described above. Phrenic nerve conduction studies were performed with single stimulation (0.5 ms duration; 6 mV amplitude) at the neck via near nerve needle electrodes placed along the phrenic nerve.[10,51] The ground needle

electrode was placed in the tail, and the reference electrode was placed subcutaneously in the right abdominal region. Recording was obtained via a surface strip along the costal margin of the diaphragm, and CMAP amplitude was measured baseline to peak. Recordings were made using an ADI Powerlab 8/30 stimulator and BioAMP amplifier (ADInstruments, Colorado Springs, CO), followed by computer-assisted data analysis (Scope 3.5.6, ADInstruments). For each animal, 10–20 tracings were averaged to ensure reproducibility.

Spontaneous EMG recordings. Prior to being euthanized, animals received a laparotomy. These EMG recordings were terminal experiments and were only conducted immediately prior to euthanasia. Bipolar electrodes spaced by 3 mm were inserted into specific subregions in the right hemidiaphragm (*i.e.*, dorsal, medial, or ventral regions). Activity was recorded and averaged during spontaneous breathing at each of these three locations separately in each animal. The EMG signal was amplified, filtered through a band-pass filter (50–3,000 Hz), and integrated using LabChart 7 software (ADInstruments). Parameters such as inspiratory bursts per minute, discharge duration and integrated peak amplitude were averaged over 2 minute sample periods. No attempt was made to control or monitor the overall level of respiratory motor drive during the EMG recordings.

Statistics. Results were expressed as means ± standard error of the mean (SEM). A Kolmogorov–Smirnov test was conducted for all variables to assess normality. Unpaired *t*-test or Mann–Whitney was used to assess statistical significance between two groups. With respect to multiple comparisons involving three groups or more, statistical significance was assessed by analysis of variance (one-way ANOVA) followed by *post hoc* test (Bonferroni's method). Statistics were computed with Graphpad Prism 5 (GraphPad Software, La Jolla, CA). $P < 0.05$ was considered as statistically significant.

ACKNOWLEDGMENTS

This work was supported by the Craig H Neilsen Foundation (grant #190140 to A.C.L.), the Morton Cure Paralysis Fund (to A.C.L.) and the NINDS (grant #1R01NS079702 to A.C.L.). K.L. (Sidney Medical College at Thomas Jefferson University): Conception and design, collection and/or assembly of data, data analysis and interpretation, manuscript writing. E.J. (Sidney Medical College at Thomas Jefferson University): Collection and/or assembly of data, data analysis and interpretation. T.J.H. (Sidney Medical College at Thomas Jefferson University): Collection and/or assembly of data, data analysis and interpretation. D.S. (Sidney Medical College at Thomas Jefferson University): Collection and/or assembly of data, data analysis and interpretation. K.A.R. (Sidney Medical College at Thomas Jefferson University): Collection and/or assembly of data, data analysis and interpretation. N.J.M. (Johns Hopkins University School of Medicine): Provision of study material or patients, data analysis and interpretation. M.C.W. (Arcadia University): Collection and/or assembly of data, data analysis and interpretation. D.J.P. (University of Montana): Provision of study material or patients, data analysis and interpretation. A.C.L. (Sidney Medical College at Thomas Jefferson University): Conception and design, collection and/or assembly of data, data analysis and interpretation, manuscript writing, final approval of manuscript. The authors declare no competing financial interests.

REFERENCES

1. Lane, MA, Fuller, DD, White, TE and Reier, PJ (2008). Respiratory neuroplasticity and cervical spinal cord injury: translational perspectives. *Trends Neurosci* **31**: 538–547.
2. Lane, MA, Lee, KZ, Fuller, DD and Reier, PJ (2009). Spinal circuitry and respiratory recovery following spinal cord injury. *Respir Physiol Neurobiol* **169**: 123–132.
3. Zimmer, MB, Nantwi, K and Goshgarian, HG (2007). Effect of spinal cord injury on the respiratory system: basic research and current clinical treatment options. *J Spinal Cord Med* **30**: 319–330.
4. Shanmuganathan, K, Gullapalli, RP, Zhuo, J and Mirvis, SE (2008). Diffusion tensor MR imaging in cervical spine trauma. *AJNR Am J Neuroradiol* **29**: 655–659.
5. Strakowski, JA, Pease, WS and Johnson, EW (2007). Phrenic nerve stimulation in the evaluation of ventilator-dependent individuals with C4- and C5-level spinal cord injury. *Am J Phys Med Rehabil* **86**: 153–157.
6. McDonald, JW and Becker, D (2003). Spinal cord injury: promising interventions and realistic goals. *Am J Phys Med Rehabil* **82**(suppl. 10): S38–S49.
7. Park, E, Velumian, AA and Fehlings, MG (2004). The role of excitotoxicity in secondary mechanisms of spinal cord injury: a review with an emphasis on the implications for white matter degeneration. *J Neurotrauma* **21**: 754–774.
8. Maragakis, NJ and Rothstein, JD (2004). Glutamate transporters: animal models to neurologic disease. *Neurobiol Dis* **15**: 461–473.
9. Maragakis, NJ and Rothstein, JD (2006). Mechanisms of Disease: astrocytes in neurodegenerative disease. *Nat Clin Pract Neurol* **2**: 679–689.
10. Li, K, Nicaise, C, Sannie, D, Hala, TJ, Javed, E, Parker, JL *et al.* (2014). Overexpression of the astrocyte glutamate transporter GLT1 exacerbates phrenic motor neuron degeneration, diaphragm compromise, and forelimb motor dysfunction following cervical contusion spinal cord injury. *J Neurosci* **34**: 7622–7638.
11. Lepore, AC and Maragakis, NJ (2007). Targeted stem cell transplantation strategies in ALS. *Neurochem Int* **50**: 966–975.
12. Pekny, M and Nilsson, M (2005). Astrocyte activation and reactive gliosis. *Glia* **50**: 427–434.
13. Lepore, AC, Rauck, B, Dejea, C, Pardo, AC, Rao, MS, Rothstein, JD *et al.* (2008). Focal transplantation-based astrocyte replacement is neuroprotective in a model of motor neuron disease. *Nat Neurosci* **11**: 1294–1301.
14. Rao, MS, Noble, M and Mayer-Pröschel, M (1998). A tripotential glial precursor cell is present in the developing spinal cord. *Proc Natl Acad Sci USA* **95**: 3996–4001.
15. Lepore, AC, O'Donnell, J, Kim, AS, Yang, EJ, Tuteja, A, Haidet-Phillips, A *et al.* (2011). Reduction in expression of the astrocyte glutamate transporter, GLT1, worsens functional and histological outcomes following traumatic spinal cord injury. *Glia* **59**: 1996–2005.
16. Regan, MR, Huang, YH, Kim, YS, Dykes-Hoberg, MI, Jin, L, Watkins, AM *et al.* (2007). Variations in promoter activity reveal a differential expression and physiology of glutamate transporters by glia in the developing and mature CNS. *J Neurosci* **27**: 6607–6619.
17. Perego, C, Vanoni, C, Bossi, M, Massari, S, Basudev, H, Longhi, R *et al.* (2000). The GLT-1 and GLAST glutamate transporters are expressed on morphologically distinct astrocytes and regulated by neuronal activity in primary hippocampal cocultures. *J Neurochem* **75**: 1076–1084.
18. Nicaise, C, Frank, DM, Hala, TJ, Authelet, M, Pochet, R, Adriaens, D *et al.* (2013). Early phrenic motor neuron loss and transient respiratory abnormalities after unilateral cervical spinal cord contusion. *J Neurotrauma* **30**: 1092–1099.
19. Maragakis, NJ, Rao, MS, Llado, J, Wong, V, Xue, H, Pardo, A *et al.* (2005). Glial restricted precursors protect against chronic glutamate neurotoxicity of motor neurons *in vitro*. *Glia* **50**: 145–159.
20. Wright, MC, Cho, WJ and Son, YJ (2007). Distinct patterns of motor nerve terminal sprouting induced by ciliary neurotrophic factor vs. botulinum toxin. *J Comp Neurol* **504**: 1–16.
21. Wright, MC, Potluri, S, Wang, X, Dentcheva, E, Gautam, D, Tessler, A *et al.* (2009). Distinct muscarinic acetylcholine receptor subtypes contribute to stability and growth, but not compensatory plasticity, of neuromuscular synapses. *J Neurosci* **29**: 14942–14955.
22. Wright, MC and Son, YJ (2007). Ciliary neurotrophic factor is not required for terminal sprouting and compensatory reinnervation of neuromuscular synapses: re-evaluation of CNTF null mice. *Exp Neurol* **205**: 437–448.
23. Laskowski, MB and Sanes, JR (1987).Topographic mapping of motor pools onto skeletal muscles. *J Neurosci* **7**: 252–260.
24. Davies, JE, Huang, C, Proschel, C, Noble, M, Mayer-Proschel, M and Davies, SJ (2006). Astrocytes derived from glial-restricted precursors promote spinal cord repair. *J Biol* **5**: 7.
25. Nicaise, C, Hala, TJ, Frank, DM, Parker, JL, Authelet, M, Leroy, K *et al.* (2012). Phrenic motor neuron degeneration compromises phrenic axonal circuitry and diaphragm activity in a unilateral cervical contusion model of spinal cord injury. *Exp Neurol* **235**: 539–552.
26. Xu, GY, Hughes, MG, Zhang, L, Cain, L and McAdoo, DJ (2005). Administration of glutamate into the spinal cord at extracellular concentrations reached post-injury causes functional impairments. *Neurosci Lett* **384**: 271–276.
27. Xu, GY, Hughes, MG, Ye, Z, Hulsebosch, CE and McAdoo, DJ (2004). Concentrations of glutamate released following spinal cord injury kill oligodendrocytes in the spinal cord. *Exp Neurol* **187**: 329–336.
28. Hulsebosch, CE (2008). Gliopathy ensures persistent inflammation and chronic pain after spinal cord injury. *Exp Neurol* **214**: 6–9.
29. Gwak, YS, Kang, J, Unabia, GC and Hulsebosch, CE (2012). Spatial and temporal activation of spinal glial cells: role of gliopathy in central neuropathic pain following spinal cord injury in rats. *Exp Neurol* **234**: 362–372.
30. Davies, JE, Pröschel, C, Zhang, N, Noble, M, Mayer-Pröschel, M and Davies, SJ (2008). Transplanted astrocytes derived from BMP- or CNTF-treated glial-restricted precursors have opposite effects on recovery and allodynia after spinal cord injury. *J Biol* **7**: 24.
31. Davies, SJ, Shih, CH, Noble, M, Mayer-Proschel, M, Davies, JE and Proschel, C (2011). Transplantation of specific human astrocytes promotes functional recovery after spinal cord injury. *PLoS ONE* **6**: e17328.
32. Haas, C, Neuhuber, B, Yamagami, T, Rao, M and Fischer, I (2012). Phenotypic analysis of astrocytes derived from glial restricted precursors and their impact on axon regeneration. *Exp Neurol* **233**: 717–732.
33. Lepore, AC, Bakshi, A, Swanger, SA, Rao, MS and Fischer, I (2005). Neural precursor cells can be delivered into the injured cervical spinal cord by intrathecal injection at the lumbar cord. *Brain Res* **1045**: 206–216.
34. Lepore, AC and Fischer, I (2005). Lineage-restricted neural precursors survive, migrate, and differentiate following transplantation into the injured adult spinal cord. *Exp Neurol* **194**: 230–242.
35. Lepore, AC, Han, SS, Tyler-Polsz, CJ, Cai, J, Rao, MS and Fischer, I (2004). Differential fate of multipotent and lineage-restricted neural precursors following transplantation into the adult CNS. *Neuron Glia Biol* **1**: 113–126.
36. Lepore, AC, Neuhuber, B, Connors, TM, Han, SS, Liu, Y, Daniels, MP *et al.* (2006). Long-term fate of neural precursor cells following transplantation into developing and adult CNS. *Neuroscience* **139**: 513–530.
37. Cao, Q, Xu, XM, Devries, WH, Enzmann, GU, Ping, P, Tsoulfas, P *et al.* (2005). Functional recovery in traumatic spinal cord injury after transplantation of

multineurotrophin-expressing glial-restricted precursor cells. *J Neurosci* **25**: 6947–6957.
38. Hill, CE, Proschel, C, Noble, M, Mayer-Proschel, M, Gensel, JC, Beattie, MS *et al.* (2004). Acute transplantation of glial-restricted precursor cells into spinal cord contusion injuries: survival, differentiation, and effects on lesion environment and axonal regeneration. *Exp Neurol* **190**: 289–310.
39. Takahashi, K, Tanabe, K, Ohnuki, M, Narita, M, Ichisaka, T, Tomoda, K *et al.* (2007). Induction of pluripotent stem cells from adult human fibroblasts by defined factors. *Cell* **131**: 861–872.
40. Bleakman, D, Alt, A and Nisenbaum, ES (2006). Glutamate receptors and pain. *Semin Cell Dev Biol* **17**: 592–604.
41. Gensel, JC, Tovar, CA, Hamers, FP, Deibert, RJ, Beattie, MS and Bresnahan, JC (2006). Behavioral and histological characterization of unilateral cervical spinal cord contusion injury in rats. *J Neurotrauma* **23**: 36–54.
42. Sandrow, HR, Shumsky, JS, Amin, A and Houle, JD (2008). Aspiration of a cervical spinal contusion injury in preparation for delayed peripheral nerve grafting does not impair forelimb behavior or axon regeneration. *Exp Neurol* **210**: 489–500.
43. Aguilar, RM and Steward, O (2010). A bilateral cervical contusion injury model in mice: assessment of gripping strength as a measure of forelimb motor function. *Exp Neurol* **221**: 38–53.
44. Wrathall, JR, Choiniere, D and Teng, YD (1994). Dose-dependent reduction of tissue loss and functional impairment after spinal cord trauma with the AMPA/kainate antagonist NBQX. *J Neurosci* **14**(11 Pt 1): 6598–6607.
45. Nicaise, C, Putatunda, R, Hala, TJ, Regan, KA, Frank, DM, Brion, JP *et al.* (2012). Degeneration of phrenic motor neurons induces long-term diaphragm deficits following mid-cervical spinal contusion in mice. *J Neurotrauma* **29**: 2748–2760.
46. Gregori, N, Pröschel, C, Noble, M and Mayer-Pröschel, M (2002). The tripotential glial-restricted precursor (GRP) cell and glial development in the spinal cord: generation of bipotential oligodendrocyte-type-2 astrocyte progenitor cells and dorsal-ventral differences in GRP cell function. *J Neurosci* **22**: 248–256.
47. Zolotukhin, S, Byrne, BJ, Mason, E, Zolotukhin, I, Potter, M, Chesnut, K *et al.* (1999). Recombinant adeno-associated virus purification using novel methods improves infectious titer and yield. *Gene Ther* **6**: 973–985.
48. Cherry, SR, Biniszkiewicz, D, van Parijs, L, Baltimore, D and Jaenisch, R (2000). Retroviral expression in embryonic stem cells and hematopoietic stem cells. *Mol Cell Biol* **20**: 7419–7426.
49. Lepore, AC, O'Donnell, J, Kim, AS, Williams, T, Tuteja, A, Rao, MS *et al.* (2011). Human glial-restricted progenitor transplantation into cervical spinal cord of the SOD1 mouse model of ALS. *PLoS ONE* **6**: e25968.
50. Lepore, AC and Maragakis, NJ (2011). Stem cell transplantation for spinal cord neurodegeneration. *Methods Mol Biol* **793**: 479–493.
51. Lepore, AC, Tolmie, C, O'Donnell, J, Wright, MC, Dejea, C, Rauck, B *et al.* (2010). Peripheral hyperstimulation alters site of disease onset and course in SOD1 rats. *Neurobiol Dis* **39**: 252–264.